Relationship of Actin and Tubulin Distribution to Bud Growth in Wild-type and Morphogenetic-Mutant *Saccharomyces cerevisiae*

ALISON E. M. ADAMS and JOHN R. PRINGLE
Department of Cellular and Molecular Biology, Division of Biological Sciences, The University of Michigan, Ann Arbor, Michigan 48109

ABSTRACT The distribution of actin in wild-type cells and in morphogenetic mutants of the budding yeast *Saccharomyces cerevisiae* was explored by staining cells with fluorochrome-labeled phallotoxins after fixing and permeabilizing the cells by several methods. The actin appeared to be localized in a set of cortical spots or patches, as well as in a network of cytoplasmic fibers. Bundles of filaments that may possibly correspond to the fibers visualized by fluorescence were observed with the electron microscope.

The putative actin spots were concentrated in small and medium-sized buds and at what were apparently the sites of incipient bud formation on unbudded cells, whereas the putative actin fibers were generally oriented along the long axes of the mother-bud pairs. In several morphogenetic mutants that form multiple, abnormally elongated buds, the actin patches were conspicuously clustered at the tips of most buds, and actin fibers were clearly oriented along the long axes of the buds. There was a strong correlation between the occurrence of active growth at particular bud tips and clustering of actin spots at those same tips. Near the end of the cell cycle in wild-type cells, actin appeared to concentrate (as a cluster of spots or a band) in the neck region connecting the mother cell to its bud.

Observations made using indirect immunofluorescence with a monoclonal anti-yeast-tubulin antibody on the morphogenetic mutant *cdc4* (which forms multiple, abnormally elongated buds while the nuclear cycle is arrested) revealed the surprising occurrence of multiple bundles of cytoplasmic microtubules emanating from the one duplicated spindle-pole body per cell. It seems that most or all of the buds contain one or more of these bundles of microtubules, which often can be seen to extend to the very tips of the buds.

These observations are consistent with the hypotheses that actin, tubulin, or both may be involved in the polarization of growth and localization of cell-wall deposition that occurs during the yeast cell cycle.

The cell-division cycle of the yeast *Saccharomyces cerevisiae* includes the following sequential morphogenetic events (see references 16, 71, and references cited therein): (*a*) selection of a nonrandom site at which budding will occur; (*b*) formation of a ring of chitin (the "bud scar") in the largely nonchitinous cell wall at that site; (*c*) localization of new cell-wall growth to the region bounded by the chitin ring, resulting in the appearance and selective growth of a bud; (*d*) localization of new cell-wall growth to the tip of the growing bud; (*e*) cytokinesis and the formation of septal cell wall. In addition, it seems that periods of uniform growth of the bud cell wall precede and follow the period of tip growth; presumably, the relative amounts of tip growth and of uniform growth are adjusted to yield the normal ellipsoidal shape of the daughter cell (21). In addition, when the bud is largely grown, the nucleus migrates from a position within the mother cell into the neck connecting mother and bud, and the spindle becomes oriented in such a way that the ensuing nuclear division results in mother and bud each receiving one daughter nucleus (11, 32).

It seems likely that formed cytoskeletal elements play important roles in such morphogenetic events in yeast, as they

appear to do in other eucaryotes. However, only limited information has been available about the distribution and functions of cytoskeletal elements in yeast. The distribution of microtubules has been extensively studied by electron microscopy (10–13, 46, 51, 52, 60). Microtubules are both intranuclear (forming the spindle; note that the nuclear envelope does not break down during mitosis) and cytoplasmic. These two sets of microtubules emanate from the nucleoplasmic and cytoplasmic faces of the spindle-pole body, a structure embedded in the nuclear envelope. The spindle microtubules are presumably involved in chromosome separation and/or in the nuclear elongation that precedes division, although the details of this involvement are by no means clear (11, 46). On the other hand, positional correlations in normal and centrifugally perturbed cells have suggested that the cytoplasmic microtubules may be involved in the selection of the budding site and/or in directing secretory vesicles to that site and into the growing bud (10–13).

In contrast, there has been essentially no information about the distribution and function of actin-containing structures in *Saccharomyces*. Nonetheless, it is clear that this yeast contains a single, essential actin gene (25, 54, 69) and substantial quantities of actin (28, 47, 79). The possibility has been entertained that this actin might be a constituent of the ring of 10-nm diameter filaments that lies immediately subjacent to the plasma membrane in the region of the neck connecting the mother cell and bud; however, no evidence to support this possibility has been obtained (14). Although the ring of 10-nm filaments disappears shortly before cytokinesis (11, 14), the location of these filaments and the observation that they are lacking in mutants from four different complementation groups that are defective in cytokinesis (15) have suggested that the 10-nm filaments may play a positive role in this process (11, 14, 15).

In this study and its companion (see reference 44), the distribution of actin in wild-type *Saccharomyces* and in morphogenetic mutants of this yeast was examined using fluorescent phallotoxin probes, immunofluorescence, and electron microscopy. In addition, immunofluorescence has provided new evidence about the localization of cytoplasmic microtubules in relation to the budding cycle. The results are suggestive as to possible roles of the microtubules and of the actin network in the morphogenetic events described above. The results also demonstrate an expanded capability for morphological analysis of yeasts that should help to make these genetically tractable organisms an even more attractive object for studies of fundamental problems in cell biology.

A preliminary report of some of this work has been presented (63).

MATERIALS AND METHODS

Materials: 7-nitrobenz-2-oxa-1,3-diazole-phallacidin (NBD-phallacidin)[1] was obtained from L. Barak (2). Fluorescein-isothiocyanate-conjugated phalloidin (FITC-phalloidin) and tetramethylrhodaminyl-phalloidin (Rh-phalloidin) were gifts from Dr. T. Wieland (22, 87). Unlabeled phalloidin was a gift from L. Barak (via Conrad Yocum). All phallotoxins were stored at −20°C in methanol. FITC-conjugated concanavalin A (FITC-Con A) was purchased from EY Laboratories (San Mateo, CA). Rat monoclonal anti-yeast-tubulin antibody (YOL1/34) was a gift from J. Kilmartin (45). FITC-conjugated rabbit anti-rat-

---

[1] *Abbreviations used in this paper.* BSA, bovine serum albumin; Con A, concanavalin A; FITC, fluorescein isothiocyanate; NBD, 7-nitrobenz-2-oxa-1,3-diazole; PBS, phosphate-buffered saline; Rh, tetramethylrhodaminyl; *ts*, temperature-sensitive.

IgG antiserum, p-phenylenediamine, Triton X-100, poly-L-lysine hydrobromide (molecular weight ~400,000), and bovine serum albumin fraction V (BSA) were purchased from Sigma Chemical Co. (St. Louis, MO). 8-well multitest slides (U.K. cat. no. 60-408-05) were purchased from Flow Laboratories (McLean, VA), Glusulase from Endo Laboratories (Wilmington, DE), and Zymolyase 5000 from Miles Laboratories (Elkhart, IN). Giemsa stain was obtained from Fisher (Detroit, MI), bisbenzimide from Aldrich (Milwaukee, WI), and CsCl (technical grade) from Kawecki Berylco (Reading, PA). Osmium tetroxide, uranyl acetate, Spurr embedding medium, and lead citrate were purchased from Polysciences Inc. (Warrington, PA), and 50% glutaraldehyde, biological grade, was purchased from MCB (Cincinnati, OH). 0.5% Formvar in ethylene dichloride was purchased from E. F. Fullam (Schenectady, NY), 0.4-×-2-mm slotted copper grids from T. Pella (Tustin, CA), and Diafine from Acufine (Chicago, IL). Other chemicals used were reagent grade.

Genetic Methods, Yeast Strains, and Culture Conditions: Standard genetic methods (68) were used for all crosses and complementation analyses in this study. The wild-type and mutant strains used are listed in Table I.

Mutant strains JPT194, JPT23, and JPTA1493 were isolated from strains C276-4A, C276-4A, and C276-4B, respectively, after mutagenesis with ethylmethane sulfonate (24) to ~2% survival, using a screening procedure similar to that of Hartwell et al. (35). Backcrossing to C276-4B and C276-4A revealed 2:2 segregations of temperature sensitivity in essentially all tetrads, indicating that each of the mutants carries a single, nuclear, temperature-sensitive (*ts*) mutation (data not shown). At 36°C, all *ts* segregants from these crosses formed the multibudded cells typical of mutant strains defective in gene *CDC3, CDC10, CDC11,* or *CDC12* (31, 35, 61). Indeed, JPT194 showed no detectable complementation with tester strains carrying the *cdc11-1* mutation, whereas JPT23 and JPTA1493 both failed to complement tester strains carrying the *cdc12-1* mutation. In contrast, all three mutants complemented well with testers carrying mutations in other *CDC* genes. Crosses of JPT194 to a *cdc11-1* strain, of JPT23 to a *cdc12-1* strain, and of JPT23 to JPTA1493 yielded no Ts⁺ segregants in about 20 tetrads analyzed for each cross. Thus, JPT194 harbors a *ts cdc11* mutation, whereas JPT23 and JPTA1493 carry *ts cdc12* mutations. As these mutants were isolated independently of the five *cdc11* mutants and four *cdc12* mutants reported previously (35), the mutant alleles are designated *cdc11-6, cdc12-5,* and *cdc12-6,* respectively (Table I).

Cultures were grown in the rich, glucose-containing medium YM-P (49) unless otherwise noted. In some experiments, the acetate-containing growth medium AC-1 (49) was used with no supplemental carbon sources. All cultures were incubated in Erlenmeyer flasks with rotary shaking (~170 rpm), either at room temperature (24 ± 1°C) or in a water bath held at 36 ± 1°C.

Staining with Fluorochrome-labeled Phallotoxins: Unless otherwise noted, the following procedure was used. Approximately 1–3 × 10⁸ exponentially growing cells (at about 10⁷ cells/ml) or *cdc* mutant cells blocked in the cell cycle at 36°C (but continuing to grow at ~5 × 10⁶ cells/ml) were harvested by centrifugation, washed once in distilled water, and fixed in 5 ml of solution B (35 mM potassium phosphate buffer, pH 6.8, to which MgCl₂ was added to 0.5 mM) plus 0.6 ml 37% formaldehyde for 2 h at 24°C. The cells were then washed twice in distilled water and resuspended in 2 ml of phosphate-buffered saline (PBS) (diluted before use from a 20-times stock solution containing [per liter] 160 g NaCl, 4 g KCl, 22.8 g Na₂HPO₄, 4 g KH₂PO₄, and adjusted to pH 7.3 with 10 N NaOH). 200 μl of cell suspension was then stained with 1.5 μM Rh-phalloidin by adding 1 μl of a stock solution containing 0.4 mg/ml Rh-phalloidin in methanol and incubating for 2–3 h at 24°C. This and all other procedures using fluorochromes for staining were carried out in the dark. The cells were then washed five times with PBS by centrifugation, and the cell pellet was finally resuspended in a drop of mounting medium. This medium was prepared by a modification of the method of Johnson and de C. Nogueira Araujo (42): 100 mg of p-phenylenediamine was dissolved in 10 ml PBS and the solution was adjusted to pH 9 with 0.1 N NaOH; 90 ml of glycerol was then mixed in. As noted previously (42), it is essential to store the mounting medium at −20°C in the dark.

In some experiments, cells were permeabilized with detergent alone. Cells were harvested and washed as described above, then resuspended in 1 ml of 0.2% Triton X-100 in PBS plus 5 μl of the stock solution of Rh-phalloidin. After 20 min, the cells were centrifuged and then washed twice in PBS to remove detergent. Finally, the cells were resuspended to 200 μl in PBS and were further stained with 1 μl of the stock solution of Rh-phalloidin, washed, and mounted as described above.

In other experiments, cells were permeabilized by fixation, followed by digestion of the cell walls, and finally treatment with detergent. Cells were harvested, washed, and treated with formaldehyde as described above, but following fixation, the cells were centrifuged and then washed three times in solution C (solution B with sorbitol added to 1.2 M). The cells were then incubated in 55 μl Glusulase plus 1 ml solution C for 2 h at 36°C. Next, the cells were washed twice in solution C and then resuspended in 3 ml of 0.2%

TABLE I

Saccharomyces cerevisiae Strains Used in this Study

Strain*	Relevant genotype[‡]		Source (reference)	Strain*	Relevant genotype[‡]		Source (reference)
C276	a/α	(Ts⁺, prototrophic)	J. Pringle (84)	JPTA1493-H01	a/α	cdc12-6/cdc12-6	[§]
C276-4A	a	(Ts⁺, prototrophic)	J. Pringle (84)	JPT19	a	cdc24-4	J. Pringle (71)
C276-4B	α	(Ts⁺, prototrophic)	J. Pringle (84)	JPT19-H05	a/α	cdc24-4/cdc24-4	[§]
314-D5	a/α	cdc4-1/cdc4-1	L. Hartwell (30, 35)	5011-D6-J2D	a	cdc24-1	J. Pringle (71)
104	a	cdc3-1 cdc43-1	L. Hartwell (31, 35)[§]	5011-H01	a/α	cdc24-1/cdc24-1	[§]
LH104-H01	a/α	cdc3-1/cdc3-1	[§]	JPT163	a	cdc42-1	J. Pringle[¶]
17012	a	cdc10-1	L. Hartwell (31, 35)	JTP163-H01	a/α	cdc42-1/cdc42-1	[¶,§]
17012-D8	a/α	cdc10-1/cdc10-1	L. Hartwell (31)	D6	α	ρ⁺	P. Perlman (73)
LH17012-H01	a/α	cdc10-1/cdc10-1	[§]	D6ρ°	α	ρ°	P. Perlman**
332	a	cdc11-1	L. Hartwell (31, 35)	5-4/4	α	ρ⁺	P. Perlman (73)
332-D2	a/α	cdc11-1/cdc11-1	L. Hartwell (31)	5-4/4ρ°	α	ρ°	P. Perlman**
JPT194	a	cdc11-6	see text	N123	a	ρ⁺	P. Perlman (73)
JPT194-H01	a/α	cdc11-6/cdc11-6	[§]	N123ρ°	a	ρ°	P. Perlman**
471	a	cdc12-1	L. Hartwell (31, 35)	CP1AB-1AA	a/a	(Diploid)	C. Paquin (58)
LH471BD1-1A	α	cdc12-1	[‖]	CP1AB-1BB	α/α	(Diploid)	C. Paquin (58)
JPT23	a	cdc12-5	see text	JPQP1	a/a/α/α	(Tetraploid)	[††]
JPTA1493	α	cdc12-6	see text				

* All strains were maintained as deep-frozen stocks as described previously (62).
‡ Most of these strains also carry nutritional markers that are not listed here.
§ To construct the homozygous mutant diploids LH17012-H01, JPT194-H01, JPTA1493-H01, and JPT163-H01, each of the mutant strains 17012, JPT194, JPTA1493, and JPT163 was crossed with C276-4A or C276-4B, and appropriate ts segregants were then crossed again to C276-4A or C276-4B. (Because of the presumed isogenicity of C276-4A and C276-4B [84], these crosses can be regarded as backcrosses.) Homozygous diploids were then isolated after mating appropriate segregants from the second backcrosses. Strains 5011-H01, JPT19-H05, and LH104-H01 were constructed similarly from mutants 5011-D6-J2D, JPT19, and 104, except that five, five, and four successive backcrosses, respectively, were carried out before mating appropriate segregants and isolating diploid clones. From the first backcross of 104, an excess of ts segregants, only some of which gave rise to multibudded cells at 36°C, reflected the segregation of the cdc3 and cdc43 ts mutations present in 104 (35, 61; A. Adams, B. Sloat, and J. Pringle, manuscript in preparation). Further backcrossing of an appropriate segregant from this first backcross yielded tetrads showing 2:2 segregations for temperature-sensitivity, and all ts segregants produced multibudded cells at 36°C. Thus, each of these segregants carries a single, nuclear, ts mutation in gene CDC3.
‖ LH471BD1-1A is an α ts segregant obtained from a cross of 471 with C276-4B.
¶ See reference 61; also A. Adams, B. Sloat and J. Pringle, manuscript in preparation.
** To verify that these putative ρ° strains really lack mitochondrial DNA (mtDNA), we determined that they were unable to grow in AC-1 medium (where acetate is the principal carbon source), whereas the corresponding ρ⁺ parent strains grew well in this medium. Also, we asked whether mtDNA could be isolated from these strains, using the procedure of Hudspeth et al. (40). As expected, the three ρ⁺ strains all gave rise to two clear bands on bisbenzimide-CsCl gradients (one band corresponding to mtDNA and the other to contaminating nuclear DNA), whereas the three ρ° strains each yielded just a single band (in a position corresponding to that for nuclear DNA).
†† This strain was obtained by mating CP1AB-1AA with CP1AB-1BB and isolating a clone that was able to sporulate.

Triton X-100 in PBS. After 10 min, the cells were centrifuged, washed twice in PBS, and resuspended in 600 μl PBS. They were then stained with 3 μl of the stock solution of Rh-phalloidin, washed, and mounted as before.

When NBD-phallacidin or FITC-phalloidin was used to stain cells, the procedures for preparing the cells were identical to those just described, but the concentrations of labeled phallotoxins were different: NBD-phallacidin was used at ~550 nM, whereas an appropriate concentration of FITC-phalloidin was determined empirically by trial dilutions from a stock of unknown concentration. In addition, p-phenylenediamine was not used with NBD-phallacidin, as it did not appreciably retard the rapid photobleaching of this substance.

Double Staining with FITC-Con A and Rh-Phalloidin: An exponentially growing population of strain LH17012-H01, JPT194-H01, or 314-D5 was shifted from 24°C to 36°C at a cell density of ~4 × 10⁶ cells/ml. After 3–4 h at 36°C, 1 ml of the culture was centrifuged and washed once in solution D (10 mM sodium phosphate buffer, pH 7.2, to which NaCl was added to 150 mM) at 36°C. The cells were then incubated at 36°C in 1.5 ml of solution D to which 0.15 ml of the 1 mg/ml FITC-Con A stock had been added. After 30 min, the cell suspension was diluted into 50 ml of fresh growth medium that had been prewarmed to 36°C. Hence, the cells were allowed to resume growth at 36°C in the presence of a much-reduced concentration of unbound FITC-Con A. After 30–40 min of incubation under these conditions, 6 ml of 37% formaldehyde was added to the culture. After 30 min, the cells were collected by centrifugation, washed twice in PBS, and resuspended in 400 μl PBS plus 2 μl of the stock solution (see above) of Rh-phalloidin. After 30 min, the cells were centrifuged and washed twice in PBS, and the pellet was resuspended in mounting medium as described above.

Staining with Anti-Yeast-Tubulin Antibody: Three procedures were employed. In the first, cells were permeabilized with formaldehyde, Glusulase, and Triton X-100 as described above in reference to staining with phallotoxins. They were then incubated for 1.5 h at 24°C in a rat monoclonal anti-yeast-tubulin antibody preparation diluted as described in reference 44. After washing, the cells were incubated for 1.5 h at 24°C in appropriately

diluted FITC-conjugated rabbit anti-rat-IgG antiserum. After washing again, the cells were resuspended in a drop of mounting medium as described above. The second procedure was similar to the first except that the detergent treatment was omitted and the antibody incubations were carried out on cells immobilized on polylysine-coated slides (45). The third procedure was applied to *cdc* mutant cells that were more resistant to permeabilization than wild-type cells. It was similar to the second procedure except that cells were fixed initially directly in the culture medium and subsequently digested with a mixture of Glusulase and Zymolyase (*cf.* also reference 44). Full details of these procedures are available from the authors.

Fluorescence Microscopy: Cells were viewed and photographed using a Leitz Orthoplan microscope equipped for rhodamine and fluorescein epi-illumination fluorescence microscopy. NBD-phallacidin-stained cells were viewed with the same filter as used for fluorescein. Some cells were also viewed and photographed in bright field, merely by switching the light source. Photographs were made on Kodak Tri-X pan film, using a 100× oil-immersion objective and a 10× photo-eyepiece. The exposure times for cells stained with Rh-phalloidin, FITC-Con A, and FITC-conjugated antibodies were 1.5 to 2 min, 3 s, and 1.5 to 2 min, respectively. Film was developed in Diafine according to the manufacturer's instructions.

Electron Microscopy: Cells were prepared for electron microscopy following the procedures of Byers and Goetsch (13; and personal communication). In some samples, 35 μM phalloidin was included in the glutaraldehyde-fixation mix. Serial sections were viewed on a Philips EM 300 operated at 60 kV.

Other Methods: Total cell numbers were estimated from absorbance measurements at 660 nm as described by Pringle and Mor (62). For nuclear staining, cells were treated with modified Helly's fixative (65), immobilized on polylysine-coated multiwell slides (as described above), stained with Giemsa (65), and photographed in bright field using a 100× objective on a Zeiss photomicroscope. Adhesion of cells to slides with polylysine rather than egg white reduced both clumping of cells and background staining, and thus

facilitated examination of individual stained cells. Time-lapse photomicroscopy was carried out as described by Hartwell et al. (34). Spheroplasts were prepared by digestion of cell walls for 2 h at 36°C with glusulase diluted 33 times with 1 M sorbitol in water.

RESULTS

Staining of Wild-type Cells with Fluorochrome-labeled Phallotoxins

Most observations of wild-type and mutant cells were made using Rh-phalloidin and mounting the cells in a medium containing p-phenylenediamine as described in Materials and Methods. Omission of the p-phenylenediamine did not change the patterns of staining observed, but the more rapid photobleaching made observation and (especially) photographic documentation difficult.

When wild-type cells were stained after fixation with formaldehyde only, or after fixation with formaldehyde followed by treatment with Glusulase and Triton X-100 (see Materials and Methods), similar patterns of fluorescence were observed (Fig. 1, A and B). Numerous small patches or spots were seen distributed over the cell surface; the cortical location of these spots was clear when the microscope was focused up and down. In addition, fibers were seen coursing through the cells, generally in a direction roughly parallel to the long axes of the cells. In unbudded cells, there was often a concentration of fluorescence near one pole (Fig. 1A, cell g), and in cells with very small buds there was generally a pronounced concentration of fluorescence in the bud (Fig. 1A, cells e and f; Fig. 1B, cell a). In both cases, the concentration of fluorescence was usually resolvable as a cluster of individual spots. In cells with medium-sized buds, there was typically a higher concentration of fluorescent spots in the bud than in the mother cell (Fig. 1A, cells a–c; Fig. 1B, cell d). Cells with very large buds often showed a concentration of fluorescence in the neck region, sometimes apparently as clusters of spots (Fig. 1B, cells b and c) and sometimes apparently as a band (Fig. 1A, cell h).

We believe that at least the cells treated with formaldehyde, Glusulase, and Triton X-100 were completely permeable to the labeled phalloidin (a small peptide of molecular weight 1,350), and thus that phalloidin-binding structures were being visualized regardless of their locations in the cells, because the same treatment allowed antibodies to penetrate to the interior of the cells. In particular, indirect immunofluorescence using antitubulin antibody in microfuge tubes (Materials and Methods, first antibody procedure) revealed microtubule structures similar to those seen using the multiwell-slide procedures (Materials and Methods, second and third antibody procedures; cf. Fig. 3C here and Figs. 3, 6, 7, and 8 of reference 44). (It should be noted that the multiwell-slide procedures are preferable for immunofluorescence as they require less antibody and the cells show less nonspecific staining.)

We investigated the minimum treatment necessary to allow labeled phallotoxins to penetrate into the cells. Live cells are apparently not permeable to the labeled phallotoxins: staining of cells that had simply been removed from the culture and washed with water revealed fluorescence in only two of 1,104 cells observed in bright field (Fig. 1, D and E). We presume that these exceptional cells had died and become permeable before staining. In contrast, either formaldehyde fixation alone or detergent treatment alone allowed staining. A 2-h fixation with formaldehyde was used routinely (Fig. 1A), but

even a 5-min fixation yielded similar staining patterns (not shown), although not all cells were stained in the latter case. The very similar (albeit usually more patchy) staining patterns observed after detergent treatment only (Fig. 1C) were displayed by only ~15% of the cells, the rest remaining unstained or very lightly stained. Although we do not know the reason for this heterogeneity, these results confirm that removal of the cell wall is not essential for staining if the membrane is permeabilized (with either formaldehyde of Triton X-100) and indicate that the staining pattern observed is not simply an artifact of formaldehyde fixation.

Additional controls indicated that neither autofluorescence nor nonspecific binding of fluorochromes contributed significantly to the staining patterns observed. Cells that were treated as those shown in Fig. 1A, except with the omission of Rh-phalloidin from the staining mixture, showed no autofluorescence (Fig. 1, F and G). To demonstrate the specificity of the staining reaction, fixed cells were preincubated with an excess of unlabeled phalloidin before the addition of Rh-phalloidin. As shown in Fig. 1, H and I, staining was dramatically reduced. Moreover, the observation that staining of cells prepared in various ways with FITC-phalloidin or NBD-phallacidin yielded the same patterns of fluorescence as observed with Rh-phalloidin (Fig. 1; FITC-phalloidin and NBD-phallacidin data not shown) also argues against the possibility that staining is due to nonspecific interactions between fluorochromes and some cellular component(s). Finally, the observation that cells converted to spheroplasts (see Materials and Methods) before fixation with formaldehyde and staining with Rh-phalloidin showed patterns of fluorescence similar to those already described is further evidence that the cortical spots are not due to interactions of the phallotoxins or fluorochromes with the cell wall.

The distribution of filaments and cortical spots was shown to be indistinguishable in strains of different ploidy (haploid, diploid, and tetraploid) and in strains carrying different alleles at MAT, the mating type locus. Thus, strains C276-4A, C276-4B, CP1AB-1AA, CP1AB-1BB, C276, and JPQP1 (Table I) all yielded identical patterns of staining. However, the patterns of staining were easier to resolve in strains of higher ploidy (hence larger cell size).

The pattern of cortical spots seen in wild-type cells is reminiscent of that seen when cells containing mitochondria are stained with the fluorescent dye DAPI (4',6-diamidino-2-phenylindole), which binds to mtDNA (85). However, three "ρ°" strains lacking mtDNA yielded patterns of spots and filaments identical to those of their wild-type "ρ^{+}" parent strains after staining with NBD-phallacidin (data not shown), making it highly unlikely that these patterns are in any way related to the presence of mitochondria or of mtDNA.

Staining with Rh-phalloidin of Morphogenetic Mutants

Yeast mutants defective in the morphogenetic events of the cell cycle (see our introduction) have been isolated by Hartwell, Pringle, and their collaborators (30–32, 34, 35, 61, 71). Three classes of these mutants were examined in this study. ts mutants defective in gene $CDC24$ or $CDC42$ are unable to bud at restrictive temperature, but continue growth and (to a variable extent) the nuclear cycle of DNA synthesis and nuclear division (32, 35, 61). Thus, these mutants arrest development as large, unbudded cells that often contain two
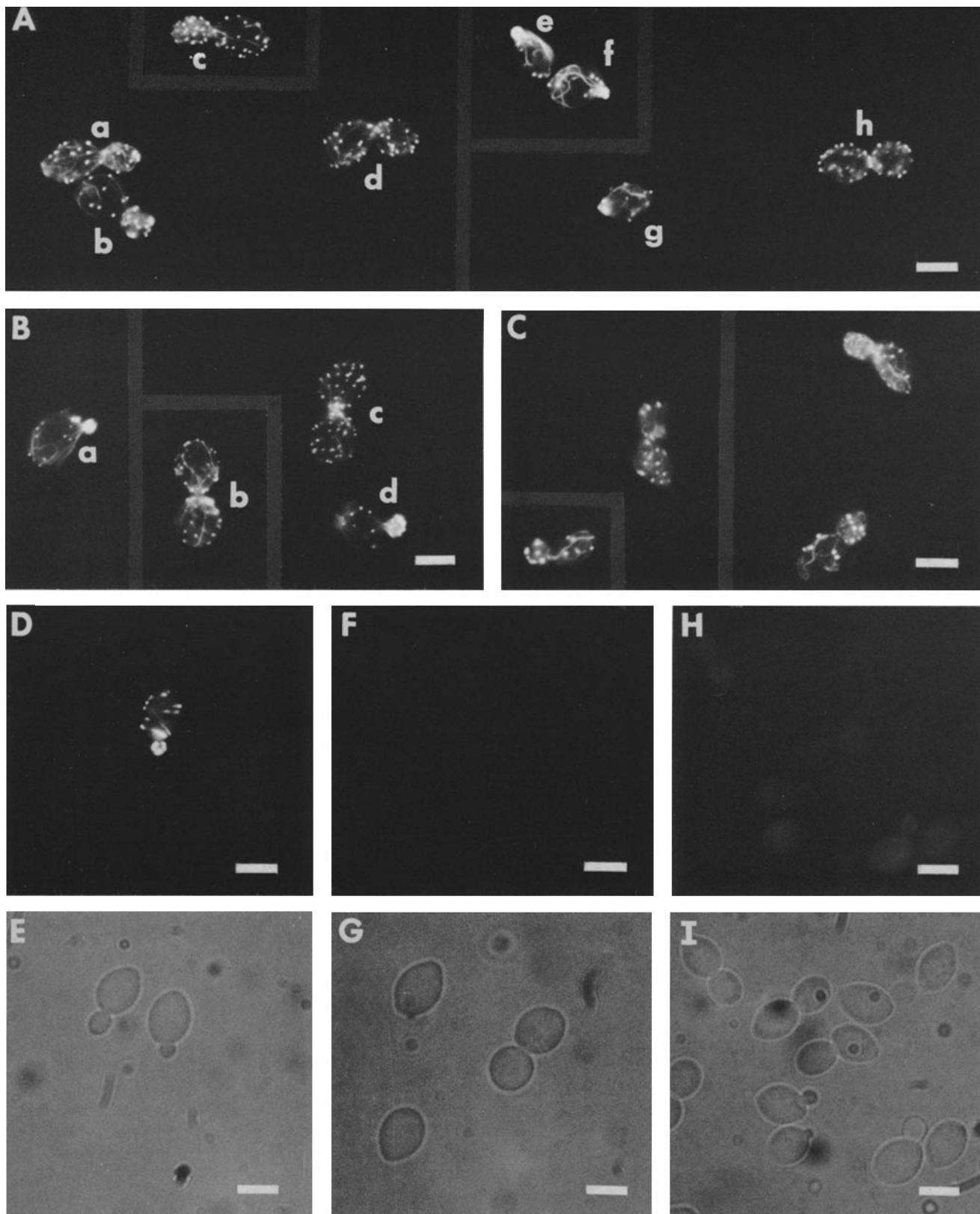
FIGURE 1 Fluorescence and bright-field micrographs of wild-type cells (strain C276), illustrating the patterns (A–E) and specificity (F–I) of staining with Rh-phalloidin. Samples were prepared and photographed as described in Materials and Methods. A–D, F, and H were photographed with the same lenses and exposure times and were printed at similar enlarger and exposure settings. (A–C) Composite fluorescence micrographs of cells permeabilized for staining by (A) fixing with formaldehyde for 2 h; (B) fixing with formaldehyde followed by treatment with Glusulase and Triton X-100; (C) treating with Triton X-100 alone. Lower-case letters identify cells referred to in the text. (D and E) Fluorescence (D) and bright-field (E) micrographs of two cells stained without prior permeabilization. (F and G) Fluorescence (F) and bright-field (G) micrographs of cells treated as those shown in A, except that Rh-phalloidin was omitted from the staining mixture. (H and I) Fluorescence (H) and bright-field (I) micrographs of formaldehyde-fixed cells in which staining by Rh-phalloidin was blocked by an excess of unlabeled phalloidin. Cells were treated as those shown in A, except that after fixation and washing, they were preincubated for 20 min at room temperature with 35 μM phalloidin before adding 1.5 μM Rh-phalloidin. The cells were then incubated an additional 2.5 h in this mixture of labeled and unlabeled phalloidin before washing and mounting by the usual procedures. Bars, 5 μm. (A–I) Approximately × 1,400.
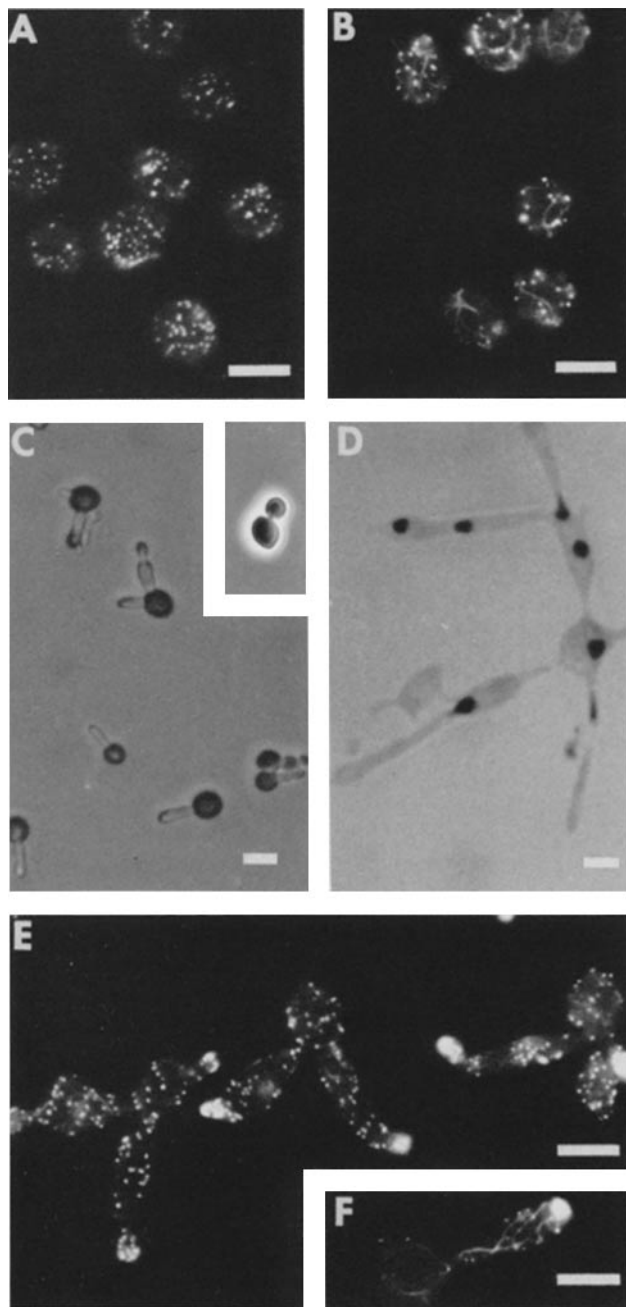
938

or more nuclei. The *cdc24* mutants are clearly defective in multiple morphogenetic events (71), and the *cdc42* mutants, although less extensively studied, appear similar (61; A. Adams, B. Sloat, and J. Pringle, manuscript in preparation). *ts* mutants defective in gene *CDC3*, *CDC10*, *CDC11*, or *CDC12* are unable to complete cytokinesis at restrictive temperature, but undergo multiple cycles of budding, DNA synthesis, and nuclear division (31, 35, 61). The buds formed are abnormally elongated (Fig. 2*C*), and the cells develop into multinucleate, quasi-mycelial forms (Fig. 2*D*). These mutants have been shown to be defective at restrictive temperature both in formation of the ring of 10-nm diameter filaments that normally lies adjacent to the cell membrane in the region of the mother-bud neck (15) and in formation of the ring of chitin that normally forms in the cell wall in this region (A. Adams and J. Pringle, manuscript in preparation). Thus, these mutants also are defective in several morphogenetic events. Finally, *ts* mutants defective in gene *CDC4* produce multiple, abnormally shaped buds in the absence of a continuing nuclear cycle, and thus arrest development as multibudded, uninucleate cells (30, 35, 61). In addition, the two spindle-pole bodies that normally move apart to form the poles of the mitotic spindle remain unseparated in the arrested mutant cells (12).

Exponentially growing populations of diploid strains defective in these genes were shifted from permissive (24°C) to restrictive (36°C) temperature, and samples were stained with Rh-phalloidin after 0, 2, and 4 h at restrictive temperature. The 0 h samples of the several strains were indistinguishable from wild-type cells grown at 24°C, except for occasional cells that had the mutant cellular morphologies. After 2 h at 36°C, the large, unbudded cells of the three *CDC24* or *CDC42* strains examined showed a rather uniform distribution of stained spots over the entire cell surface and fibers that had no apparent orientation (Fig. 2, *A* and *B*). After 4 h at 36°C, the three strains still appeared similar to each other. Many cells within each population had a rather uniform distribution of cortical spots as before, others showed more patchy arrays of spots, and still others (probably dead, based on their crinkled appearance under bright field) yielded a dull background of fluorescence and few spots. After 2 or 4 h at 36°C, most cells of the *cdc3*, *cdc10*, *cdc11*, *cdc12*, and *cdc4* strains examined had one or more elongated buds. Both the mothers and buds showed a rather uniform distribution of stained spots and fibers, except that at the tips of the majority of buds in each population were concentrations of fluorescence (Fig. 2*E*), often resolvable as clusters of spots by focusing up and down. In addition, long fibers often seemed to extend from the mother cells to the tips of the buds (Fig. 2*F*).

Double Staining of Mutant Cells with FITC-Con A and Rh-phalloidin

On the assumption that staining of yeast with fluorochrome-labeled phallotoxins indeed reveals the intracellular distribution of actin (see Discussion), then the patterns of staining in wild-type (Fig. 1, *A* and *B*; see also reference 44) and mutant cells (Fig. 2, *E* and *F*) suggest that the actin

FIGURE 2 Fluorescence and bright-field micrographs of *ts* morphogenetic mutants after growth at restrictive temperature. The samples were prepared and photographed as described in Materials and Methods. (*A* and *B*) Fluorescence micrographs of strains (*A*) JPT19-H05 (*cdc24-4/cdc24-4*) and (*B*) 5011-H01 (*cdc24-1/cdc24-1*) after staining with Rh-phalloidin. An exponentially growing population of each strain was shifted from 24°C to 36°C at a cell density of ~3 × 10⁶ cells/ml. After 2 h, a 40-ml sample of each strain was fixed and stained as described for the cells in Fig. 1*A*. Similar observations (not shown) were made with strain JPT163-H01 (*cdc42-1/cdc42-1*). (*C* and *D*) Bright-field micrographs illustrating the abnormal morphologies of cells defective in gene *CDC3*, *CDC10*, *CDC11*, or *CDC12*. (*C*) Strain 17012-D8 (*cdc10-1/cdc10-1*) after several hours growth on an agar surface at 36°C (part of a time-lapse series); the inset is a phase-contrast micrograph of wild-type cells (strain C276) to illustrate normal bud morphology. (*D*) Strain 332-D2 (*cdc11-1/cdc11-1*) stained with Giemsa after ~9 h at 36°C. (*E* and *F*) Fluorescence micrographs of strains (*E*) JPT194-H01 (*cdc11-6/cdc11-6*) and (*F*) JPTA1493-H01 (*cdc12-6/cdc12-6*) stained with Rh-phalloidin after growth at 36°C for 4 and 2 h, respectively. Samples were prepared as described above for the *cdc24* strains (*A* and *B*). Similar observations (not shown) were made with strains LH104-H01 (*cdc3-1/cdc3-1*) and LH17012-H01 (*cdc10-1/cdc10-1*), as well as with strain 314-D5 (*cdc4-1/cdc4-1*; see Fig. 3*B*). Bars, 7 μm. (*A*, *B*, *E*, and *F*) Approximately × 1,200. (*C* and *D*) Approximately × 600.

network may have a role in the polarization of cell-wall growth in budding cells (see Discussion). To explore this possibility further, we asked if there were a correlation between the presence of a high concentration of actin at a particular bud tip and the occurrence of active growth at that tip. To distinguish between growing and nongrowing tips, we employed staining of cell-wall mannan by FITC-Con A, a procedure developed by Tkacz and Lampen (77) to demonstrate the localized deposition of new mannan at the tips of growing normal buds. Thus, exponentially growing populations of strains LH17012-H01, JPT194-H01, and 314-D5 were shifted
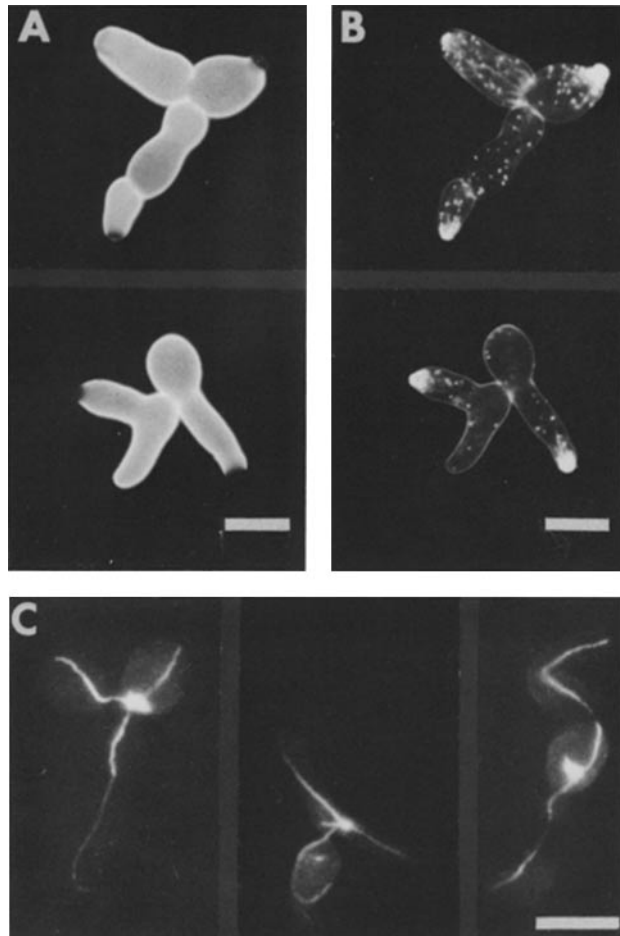

FIGURE 3 Fluorescence micrographs of strain 314-D5 (cdc4-1/cdc4-1) after growth at restrictive temperature, illustrating sites of cell-wall growth and the localization of actin and tubulin in the mutant cells. (A and B) Fluorescence micrographs of cells first stained with FITC-Con A, then allowed to resume growth in the presence of a much-reduced concentration of unbound lectin, and finally fixed and stained with Rh-phalloidin (see Materials and Methods). (A) FITC-Con A staining. Both actively growing bud tips (FITC-Con A-dark) and nongrowing bud tips (FITC-Con A-bright) are seen. (B) Rh-phalloidin staining of the cells shown in A. Focusing up and down revealed some additional spots and fibers, but no major concentrations of actin other than those visible in the micrograph. Similar observations were made (Table II) with strains LH17012-H01 (cdc10-1/cdc10-1) and JPT194-H01 (cdc11-6/cdc11-6). (C) Fluorescence micrograph of cells stained indirectly with monoclonal anti-yeast-tubulin antibody. A population growing exponentially at ~3 × 10⁶ cells/ml was shifted from 24°C to 36°C. After 4 h, the cells were prepared for staining with antibodies, using either the second or third procedure described in Materials and Methods. Bars, 7 μm. (A and B) Approximately × 1,150. (C) Approximately × 1,600.

from 24°C to 36°C, and after 3 to 4 h at restrictive temperature were exposed to FITC-Con A (see Materials and Methods). The stained cells were then allowed to resume growth at 36°C for 30–40 min in the presence of a much reduced concentration of unbound lectin, and were then fixed and stained with Rh-phalloidin. As expected, some bud tips were FITC-Con A-dark (Fig. 3A), indicating that active deposition of new (hence unstained) cell-wall material had occurred at those tips during the 30–40 min incubations after reducing the lectin concentration, while other tips were FITC-Con A-bright (Fig. 3A), indicating that no expansion of those tips had occurred since the staining with FITC-Con A. Nearly all tips that showed evidence of active growth also displayed high concentrations of actin, whereas of the tips that showed no evidence of active growth, only 24–35% stained intensely with Rh-phalloidin (Figs. 3, A and B; Table II).

Localization of Tubulin in cdc4 Mutant Cells

Frequently, individual cells of all three strains examined by staining with FITC-Con A showed evidence of active growth at two or more bud tips during the 30–40 min after diluting the lectin (Fig. 3A). Given the evidence that the spindle-pole body and extranuclear microtubules are involved in selecting the budding site and in allowing the subsequent selective growth of the bud (10–13), this observation seemed unsurprising for the cdc10 and cdc11 strains, which become multinucleate, and hence possessed of multiple spindle-pole bodies, during incubation at 36°C (Fig. 2D). However, it seemed surprising that a cdc4 strain could sustain growth of two tips simultaneously, as previous evidence has indicated that such strains arrest at 36°C with one duplicated, but unseparated, spindle-pole body per cell (12). It seemed possible that the particular subclone of strain 314-D5 used in our experiments did not behave as did the cdc4 strains studied previously. However, Giemsa staining on this subclone revealed that at least 86% of the cells were arrested with a single nucleus, while serial-section electron microscopy on a different subclone from the same (presumably homogeneous) frozen stock had revealed the expected arrest at the double-spindle-pole-body stage in ~90% of the cells examined. It also seemed possible that the multiple FITC-Con A-dark tips observed on 314-D5 cells (Fig. 3A) might have grown successively, rather than simultaneously, during the 30–40 min allowed for growth subsequent to staining with FITC-Con A. However,

TABLE II

Double-staining of Cells with FITC-Con A and Rh-phalloidin*

	Bud tips showing active growth[†]		Bud tips not showing active growth[†]	
Strain	No. of tips stained intensely with Rh-phalloidin	No. of tips not stained intensely with Rh-phalloidin	No. of tips stained intensely with Rh-phalloidin	No. of tips not stained intensely with Rh-phalloidin
314-D5	70	5	29	53
LH17012-H01	65	5	16	52
JPT194-H01	57	5	12	37

* The procedures are described in Materials and Methods. In these experiments, a variable proportion of the cells (typically ~30%) appeared totally unstained with Rh-phalloidin, and were not included in the counts.
[†] As explained in the text and illustrated in Fig. 3A, actively growing tips appear FITC-Con A-dark, while nongrowing tips appear FITC-Con A-bright.

time-lapse observations (pictures at 10-min intervals) on 314-D5 cells growing at restrictive temperature appeared to confirm that individual cells could have two or more buds elongating simultaneously. It therefore seemed of considerable interest to examine the distribution of extranuclear microtubules in multibudded 314-D5 cells by indirect immunofluorescence. The surprising result was that most such cells were found to contain two or more sets of extranuclear microtubules, apparently emanating from a single bright focus in each cell (presumably the duplicated spindle-pole body; the common origin of the sets of microtubules was especially clear when the microscope was focused up and down), and running into (and often to the very tips of) the two or more buds possessed by the cells (Fig. 3C). Unfortunately, apparent heterogeneity in the effectiveness of permeabilization and staining of these mutant cells made it impossible to determine whether every bud (and hence every growing bud) contained a set of cytoplasmic microtubules, but our observations appear compatible with this possibility. It was also not possible to do a double-label experiment with FITC-Con A and antitubulin antibody, because of the need to remove cell walls in order to achieve penetration of the cells by antibodies.

Electron Microscopic Visualization of Bundles of Filaments That May Be Actin

Although purified yeast actin polymerizes in vitro into typical filaments of ~7-nm diameter (28, 44, 47), no such filaments have been observed in the cells by electron microscopy. As the cytoplasmic fibers visualized with fluorescent phallotoxins (Figs. 1–3) and with antiactin antibodies (44) presumably represent bundles of actin filaments rather than single filaments, it seemed likely that the corresponding structures could be detected electron microscopically even against the imperfectly preserved and rather granular yeast cytoplasm. Accordingly, we carried out a search for the expected filament bundles after fixing either in the absence or the presence of phalloidin. (Treatment with phalloidin has been reported to improve the preservation of actin filaments when fixed in vitro and exposed to osmic acid [27].) Bundles of filaments (Fig. 4) were in fact found in many cells in two separate experiments. These bundles were always found in the cytoplasm, but no consistent association between them and the cell membrane or any intracellular component was detected. The filaments making up the bundles appeared to be helical and ≤10 nm in diameter. In addition, they seemed to be in register, revealing a periodicity along the long axis of the bundle that was clear in sections that had been cut parallel to the bundles. The number of successive sections in which a particular bundle was visible varied from 2 to about 15, depending largely on the angle at which the sections had been cut with respect to the direction in which the filaments were oriented. In one experiment, bundles of filaments were found in 41 of 168 cells examined. As about 1/8 of the volume of each cell was examined, on average, a typical cell must contain at least two of these filament bundles. Fixation in the presence or absence of phalloidin produced no detectable differences in the appearance or frequency of the filament bundles.

DISCUSSION

Actin Localization in Wild-type Cells

The specific binding of phallotoxins to F-actin has been

well established in other systems (2, 3, 17, 20, 22, 55, 59, 81–83, 87), and it has recently been shown that phalloidin can interact with yeast actin polymerized in vitro (28). The results presented in Fig. 1 and the associated text indicate that the patterns of fluorescence observed in yeast cells stained with fluorochrome-labeled phallotoxins are (a) due to staining with the labeled phallotoxins and not due to autofluorescence; (b) obtained only when the cells are permeabilized; (c) indistinguishable (except in the percentages of cells stained) when permeabilization is by any of several methods, including some that omit formaldehyde fixation and some that are known to permeabilize the cells and nuclei even to molecules as large as antibodies; (d) due to a specific interaction between the phallotoxin moiety and a cellular component; (e) apparently not dependent on the presence of cell wall; and (f) apparently not related to the distribution of mitochondria or their genomes. Moreover, similar staining patterns are obtained using indirect immunofluorescence with an affinity-purified anti-yeast-actin antiserum (44). Finally, the fibers observed with Rh-phalloidin disappear when a yeast mutant carrying a ts mutation in the actin gene is incubated at restrictive temperature (P. Novick, D. Shortle, and D. Botstein, personal communication). Thus, it seems virtually certain that both the phallotoxin and antibody probes are reliably revealing the intracellular distribution of actin in yeast.

The actin fibers observed in yeast appear similar to those seen in many other cell types (e.g., 2, 3, 6, 9, 17, 55, 59, 70, 80, 81, 87). The fibers are presumably bundles of individual actin filaments, and additional actin filaments may well be present (singly or in smaller bundles) but not visualized by the procedures used here (cf. reference 36). The cortical spots observed in yeast are a more unusual staining pattern for actin, although not unprecedented (see below). These spots do not disappear when the actin mutant is incubated at restrictive temperature (P. Novick, D. Shortle, and D. Botstein, personal communication), and the possibility remains open that they are an artifact of some type. However, the behavior of a single conditional mutant is not strong evidence against the conclusion that the spots contain actin, and we feel that the weight of the evidence (as summarized in the preceding paragraph) strongly supports the conclusion that the spots are a valid feature of the distribution of actin in yeast. The possible identity of these spots with the actin particles produced in response to Ca^{2+} in vitro (29) is discussed in reference 44.

Although hard evidence is lacking (see the discussion of possible fiber-to-spot connections in reference 44), we speculate that the putative actin spots correspond to sites of anchorage of the cytoplasmic network of actin filaments to the cell membrane. It is also conceivable that attachments of the cell membrane to the cell wall occur at these sites. Good evidence both for such anchorage of the actin cytoskeleton to the plasma membrane and for transmembrane attachments linking the cytoskeleton to basement membranes or other substrata has been obtained in many other systems, using a variety of techniques (e.g., 4, 5, 7–9, 26, 50, 70, 74, 75, 80). The putative attachment sites have not usually been seen as spots or patches using fluorescence microscopy with actin-specific probes. However, in transformed cells in which the actin stress fibers have disappeared or are less prominent, actin patches at the sites of cellular adhesion plaques have been observed using antiactin immunofluorescence and fluorochrome-labeled phallotoxins (6, 17, 70). Actin-specific fluo-
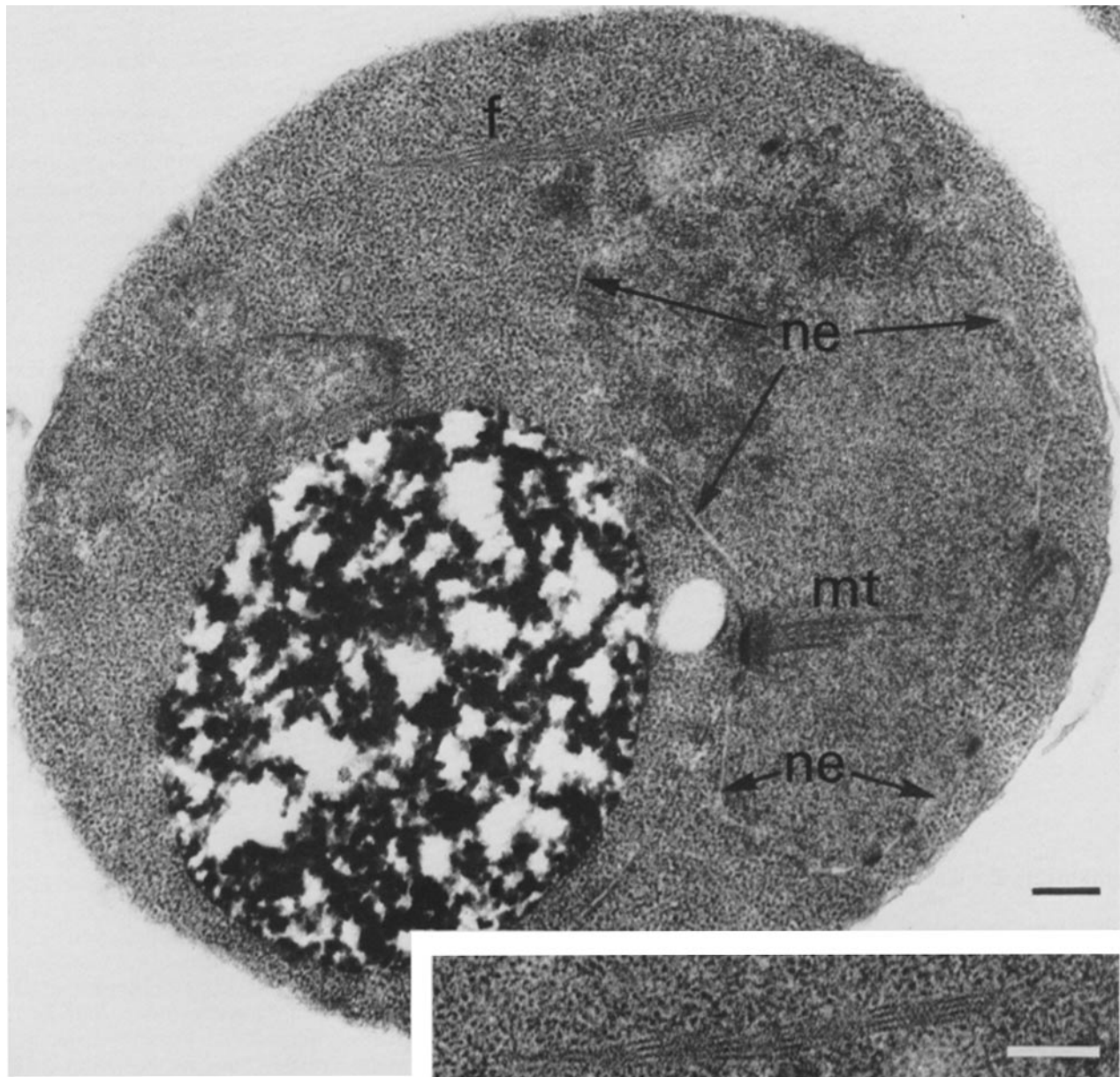
FIGURE 4   Electron micrographs of a wild-type cell (strain C276) fixed in the presence of phalloidin (see Materials and Methods). A bundle of filaments (f), located outside the nuclear envelope (ne), is shown. The diameter of the filaments is clearly less than that of the microtubules (mt) of the mitotic spindle. (Although the spindle-pole body is clearly visible in this micrograph, cytoplasmic microtubules are not.) (Inset) The same bundle of filaments at higher magnification. Bars, 200 nm. Approximately × 49,000. (Inset) Approximately × 70,000.

rescent probes have also revealed cortical patches, possibly homologous to those described here, in living and fixed mouse macrophages (1), in mouse embryo cells (48), and in the hyphae of a filamentous fungus (37).

The bundles of filaments observed electron microscopically (Fig. 4) may correspond to the fibers seen by fluorescence microscopy. Although we observed filament bundles at a frequency that would extrapolate to only about two bundles per cell (see Results), it is likely that we observed only a subset of the bundles: bundles that were oriented too nearly perpendicularly to the plane of sectioning, that contained small numbers of filaments, or that were poorly preserved during preparation for electron microscopy (27) would probably not have been detected. The morphology of these filament bundles resembles somewhat that of actin filaments arranged in "paracrystalline arrays"; such arrays have been found in a

variety of cell types (18, 19, 76) and are also formed in vitro when actin is polymerized in the presence of a high concentration of $MgCl_2$ (18, 72). A problem with this interpretation is that neither the diameter of the yeast filaments (apparently closer to 10 than to 7 nm) nor the periodicity of the striations in the yeast bundles (apparently closer to 120 than to 35 nm) corresponds well to what has been observed in other systems. However, it seems possible that differences in the actins themselves or in accessory proteins involved in polymerization could account for these discrepancies. More definite identification of the filaments observed electron microscopically in yeast as actin must await their successful decoration with myosin subfragments or with appropriate antibodies. We observed nothing with the electron microscope that appears to correspond to the putative actin spots observed by fluorescence.

No evidence was obtained for an association of actin with the 10-nm filaments of the neck region, as discussed in detail in reference 44.

Possible Role for Actin in the Localization of Secretion in Yeast

During the cell cycle of wild-type yeast cells, the bud grows while the mother cell does not (33, 43, 71), and the deposition of new cell-wall constitutents, as well as the secretion of other materials, is localized to the bud and (for much of the period of bud enlargement) to its tip (21, 23, 41, 71, 77, 78). These phenomena appear homologous to the localized growth observed at hyphal tips in mycelial fungi (21, 38, 39). This polarization of growth and localization of secretion are believed to occur primarily, if not exclusively, by means of a directed movement of one or more classes of secretory vesicles to the appropriate sites on the cell surface (11–13, 21, 39, 51, 56, 66, 67). The patterns of actin localization during the cell cycle of wild-type cells (Fig. 1 and reference 44) suggest that actin may play a role in this directed movement of secretory vesicles (see detailed discussion in reference 44); a similar suggestion has been made for hyphal fungi based on electron microscopic observations of microfilament localization (38).

The results obtained with *ts* morphogenetic mutants (Figs. 2 and 3) strongly support these suggestions. Two mutants that are defective in budding and deposit new cell-wall materials in a delocalized fashion display nonpolarized distributions of actin spots and fibers (Fig. 2, *A* and *B*). In contrast, several mutants that produce abnormally elongated buds (Fig. 2, *C* and *D*), presumably because of an exaggerated polarization of bud growth (21), also show what appears to be an exaggeration of the polarization of actin localization that is observed in wild-type cells with small and medium-sized buds (Fig. 1; reference 44). That is, actin fibers often conspicuously run the lengths of the long buds (Figs. 2*F* and 3*B*), while the putative actin spots are conspicuously clustered at the tips of most buds. Particularly convincing evidence for the suggested involvement of actin in producing polarized growth and secretion in yeast is the strong correlation between the occurrence of clusters of actin spots at particular bud tips and the occurrence of active growth at those same tips (Fig. 3, *A* and *B*; Table II; and associated text). The minority of bud tips that showed concentrations of actin but no clear evidence of active growth may well have been just beginning to grow when they were fixed; the tip at the upper left of the top cell in Fig. 3, *A* and *B*, appears to be an example, as (at least in the original photograph) it shows unmistakable, but very modest, traces of FITC-Con A-darkness to correspond to its cluster of actin. Alternatively, tip growth may well be dependent on other factors in addition to an appropriate distribution of actin. The very few (but potentially more troublesome) tips that showed clear evidence of active growth, but no demonstrable concentrations of actin, probably were inadequately stained with the Rh-phalloidin. (In addition to the cells that appeared totally unstained with Rh-phalloidin [Table II], a few cells in each of these experiments had particular buds that appeared poorly stained.) It is also possible that these tips had ceased to grow, and the actin had become redistributed, prior to fixation; recall that 30–40 min were allowed for growth after exposure to the FITC-Con A.

Possible Roles of the Cytoplasmic Microtubules

Byers and Goetsch have proposed (11–13) that the cytoplasmic microtubules are involved in the directed movement of secretory vesicles to the growing bud. This proposal was based on electron microscopic observations of normal, mutant, and centrifugally perturbed cells. In particular, bud emergence and the early stages of bud growth were found to occur in cells with duplicated, but unseparated, spindle-pole bodies. In such cells, the double spindle-pole body was always found to be oriented toward the bud site, and the cytoplasmic microtubules ran from the spindle-pole body into the bud, often seeming (at least superficially) to be associated with the secretory vesicles that were concentrated there. Similarly, both electron microscopic observations and inhibitor experiments have suggested a possible role for microtubules in the tip growth of hyphal fungi (38, 39).

The immunofluorescence observations on cytoplasmic-microtubule distribution in wild-type and mutant yeast cells significantly extend the correlations observed previously by electron microscopy, and thus appear to support the proposal of Byers and Goetsch (11–13). In particular, it is now clear that the orientation of cytoplasmic microtubules toward the bud site in wild-type cells is maintained after spindle-pole body separation and spindle formation, until the nucleus itself migrates into the bud (Fig. 3 of reference 44 and the associated text). Moreover, *cdc4* mutant cells, which produce multiple buds while arrested with a duplicated, but unseparated, spindle-pole body, appear both to be able to sustain the growth of several bud tips simultaneously (Fig. 3*A* and associated text) and to possess a discrete bundle of cytoplasmic microtubules in each growing bud (Fig. 3*C*), although it should be noted that experimental limitations (see Results) make these conclusions somewhat tentative.

A slight problem for the hypothesis of microtubule involvement in polarized growth in yeast is that the cytoplasmic microtubules in cells with short intra-mother-cell-spindles were only rarely observed to extend to the tips of the buds (44), although in such cells tip growth of the buds should be occurring (21, 41, 71, 77, 78). However, this could be a visualization problem, and it is striking that in *cdc4* cells, which show an exaggerated tip growth, the cytoplasmic microtubules usually did appear to run all the way to the tips of the buds (Fig. 3*C*).

A more serious problem for the hypothesis at issue is posed by experiments in which microtubule inhibitors have apparently arrested cell division to produce a homogeneous population of large-budded cells (64, 86), suggesting that the emergence and selective growth of the bud are independent of microtubule function. However, the evidence that cytoplasmic microtubules were indeed abolished in these studies appears inconclusive. Nonetheless, it should be noted that an alternative hypothesis as to the role of the cytoplasmic microtubules is equally compatible with the evidence from positional correlations (except possibly the observations on *cdc4*) and not in apparent conflict with the inhibitor studies just cited. That is, the cytoplasmic microtubules may be involved in the nuclear migration (into the mother-bud neck) or spindle orientation, or both, that are necessary to ensure that each daughter cell gets a nucleus during cell division. In this regard, it should be noted that strong evidence has been presented for the involvement of microtubules in nuclear migration in

Aspergillus hyphae (57). Immunofluorescence staining of cytoplasmic microtubules may assist efforts to define more precisely the roles of the cytoplasmic microtubules in yeast using inhibitors and tubulin mutants (53).

REFERENCES

1. Amato, P. A., E. R. Unanue, and D. L. Taylor. 1983. Distribution of actin in spreading macrophages: a comparative study on living and fixed cells. *J. Cell Biol.* 96:750–761.
2. Barak, L. S., and R. R. Yocum. 1981. 7-Nitrobenz-2-oxa-1,3-diazole (NBD)-phallacidin: synthesis of a fluorescent actin probe. *Anal. Biochem.* 110:31–38.
3. Barak, L. S., R. R. Yocum, E. A. Nothnagel, and W. W. Webb. 1980. Fluorescence staining of the actin cytoskeleton in living cells with 7-nitrobenz-2-oxa-1,3-diazole-phallacidin. *Proc. Natl. Acad. Sci. USA* 77:980–984.
4. Bennett, V., J. Davis, and W. E. Fowler. 1982. Brain spectrin, a membrane-associated protein related in structure and function to erythrocyte spectrin. *Nature (Lond.).* 299:126–131.
5. Birchmeier, W., T. A. Liberman, B. A. Imhof, and T. E. Kreis. 1982. Intracellular and extracellular components involved in the formation of ventral surfaces of fibroblasts. *Cold Spring Harbor Symp. Quant. Biol.* 46:755–767.
6. Boschek, C. B., B. M. Jockusch, R. R. Friis, R. Back, E. Grundmann, and H. Bauer. 1981. Early changes in the distribution and organization of microfilament proteins during cell transformation. *Cell.* 24:175–184.
7. Branton, D. 1982. Membrane cytoskeletal interactions in the human erythrocyte. *Cold Spring Harbor Symp. Quant. Biol.* 46:1–5.
8. Brown, S. S., H. L. Malinoff, and M. S. Wicha. 1983. Connectin: cell surface protein that binds both laminin and actin. *Proc. Natl. Acad. Sci. USA* 80:5927–5930.
9. Burridge, K., T. Kelly, and P. Mangeat. 1982. Nonerythrocyte spectrins: actin-membrane attachment proteins occurring in many cell types. *J. Cell Biol.* 95:478–486.
10. Byers, B. 1981. Multiple roles of the spindle pole bodies in the life cycle of *Saccharomyces cerevisiae*. *In* Molecular Genetics in Yeast. Alfred Benzon Symposium 16. D. van Wettstein, J. Friis, M. Kielland-Brandt, and A. Stenderup, editors. Munksgaard, Copenhagen. 119–131.
11. Byers, B. 1981. Cytology of the yeast life cycle. *In* The Molecular Biology of the Yeast Saccharomyces: Life Cycle and Inheritance. J. N. Strathern, E. W. Jones, and J. R. Broach, editors. Cold Spring Harbor Laboratory, Cold Spring Harbor, NY. 59–96.
12. Byers, B., and L. Goetsch. 1974. Duplication of spindle plaques and integration of the yeast cell cycle. *Cold Spring Harbor Symp. Quant. Biol.* 38:123–131.
13. Byers, B., and L. Goetsch. 1975. Behavior of spindles and spindle plaques in the cell cycle and conjugation of *Saccharomyces cerevisiae*. *J. Bacteriol.* 124:511–523.
14. Byers, B., and L. Goetsch. 1976. A highly ordered ring of membrane-associated filaments in budding yeast. *J. Cell Biol.* 69:717–721.
15. Byers, B., and L. Goetsch. 1976. Loss of the filamentous ring in cytokinesis-defective mutants of budding yeast. *J. Cell Biol.* 70(2, Pt. 2):35a. (Abstr.)
16. Cabib, E. 1975. Molecular aspects of yeast morphogenesis. *Annu. Rev. Microbiol.* 29:191–214.
17. Carley, W. W., L. S. Barak, and W. W. Webb. 1981. F-actin aggregates in transformed cells. *J. Cell Biol.* 90:797–802.
18. DeRosier, D. J., and L. G. Tilney. 1982. How actin filaments pack into bundles. *Cold Spring Harbor Symp. Quant. Biol.* 46:525–540.
19. DeRosier, D., E. Mandelkow, A. Silliman, L. Tilney, and R. Kane. 1977. Structure of actin-containing filaments from two types of non-muscle cells. *J. Mol. Biol.* 113:679–695.
20. Estes, J. E., L. A. Selden, and L. C. Gershman. 1981. Mechanism of action of phalloidin on the polymerization of muscle actin. *Biochemistry.* 20:708–712.
21. Farkaš, V. 1979. Biosynthesis of cell walls of fungi. *Microbiol. Rev.* 43:117–144.
22. Faulstich, H., H. Trischmann, and D. Mayer. 1983. Preparation of tetramethylrhodaminyl-phalloidin and uptake of the toxin into short-term cultured hepatocytes by endocytosis. *Exp. Cell Res.* 144:73–82.
23. Field, C., and R. Schekman. 1980. Localized secretion of acid phosphatase reflects the pattern of cell surface growth in *Saccharomyces cerevisiae*. *J. Cell Biol.* 86:123–128.
24. Fink, G. R. 1970. The biochemical genetics of yeast. *Methods Enzymol.* 17A:59–78.
25. Gallwitz, D. 1982. Construction of a yeast actin gene intron deletion mutant that is defective in splicing and leads to the accumulation of precursor RNA in transformed yeast cells. *Proc. Natl. Acad. Sci. USA* 79:3493–3497.

26. Geiger, B. 1982. Involvement of vinculin in contact-induced cytoskeletal interactions. *Cold Spring Harbor Symp. Quant. Biol.* 46:671–682.
27. Gicquaud, C., and A. Loranger. 1981. La phalloïdine protège la F-actine contre les effets destructeurs de l'acide osmique. II. Protection par la phalloïdine de la F-actine traitée aux aldéhydes. *Eur. J. Cell Biol.* 24:320–323.
28. Greer, C., and R. Schekman. 1982. Actin from *Saccharomyces cerevisiae*. *Mol. Cell Biol.* 2:1270–1278.
29. Greer, C., and R. Schekman. 1982. Calcium control of *Saccharomyces cerevisiae* actin assembly. *Mol. Cell Biol.* 2:1279–1286.
30. Hartwell, L. H. 1971. Genetic control of the cell division cycle in yeast. II. Genes controlling DNA replication and its initiation. *J. Mol. Biol.* 59:183–194.
31. Hartwell, L. H. 1971. Genetic control of the cell division cycle in yeast. IV. Genes controlling bud emergence and cytokinesis. *Exp. Cell Res.* 69:265–276.
32. Hartwell, L. H. 1974. *Saccharomyces cerevisiae* cell cycle. *Bacteriol. Rev.* 38:164–198.
33. Hartwell, L. H., and M. W. Unger. 1977. Unequal division in *Saccharomyces cerevisiae* and its implications for the control of cell division. *J. Cell Biol.* 75:422–435.
34. Hartwell, L. H., J. Culotti, and B. Reid. 1970. Genetic control of the cell-division cycle in yeast. I. Detection of mutants. *Proc. Natl. Acad. Sci. USA* 66:352–359.
35. Hartwell, L.H., R. K. Mortimer, J. Culotti, and M. Culotti. 1973. Genetic control of the cell division cycle in yeast. V. Genetic analysis of *cdc* mutants. *Genetics.* 74:267–286.
36. Heuser, J. E., and M. W. Kirschner. 1980. Filament organization revealed in platinum replicas of freeze-dried cytoskeletons. *J. Cell Biol.* 86:212–234.
37. Hoch, H. C., and R. C. Staples. 1983. Visualization of actin *in situ* by rhodamine-conjugated phalloin in the fungus *Uromyces phaseoli*. *Eur. J. Cell Biol.* In press.
38. Howard, R. J. 1981. Ultrastructural analysis of hyphal tip cell growth in fungi: Spitzenkörper, cytoskeleton and endomembranes after freeze-substitution. *J. Cell Sci.* 48:89–103.
39. Howard, R. J., and J. R. Aist. 1980. Cytoplasmic microtubules and fungal morphogenesis: ultrastructural effects of methyl benzimidazole-2-ylcarbamate determined by freeze-substitution of hyphal tip cells. *J. Cell Biol.* 87:55–64.
40. Hudspeth, M. E. S., D. S. Shumard, K. M. Tatti, and L. I. Grossman. 1980. Rapid purification of yeast mitochondrial DNA in high yield. *Biochim. Biophys. Acta.* 610:221–228.
41. Johnson, B. F., and E. J. Gibson. 1966. Autoradiographic analysis of regional cell wall growth of yeasts. III. *Saccharomyces cerevisiae*. *Exp. Cell Res.* 41:580–591.
42. Johnson, G. D., and G. M. de C. Nogueira Araujo. 1981. A simple method of reducing the fading of immunofluorescence during microscopy. *J. Immunol. Meth.* 43:349–350.
43. Johnston, G. C., J. R. Pringle, and L. H. Hartwell. 1977. Coordination of growth with cell division in the yeast *Saccharomyces cerevisiae*. *Exp. Cell Res.* 105:79–98.
44. Kilmartin, J. V., and A. E. M. Adams. 1983. Structural rearrangements of tubulin and actin during the cell cycle of the yeast *Saccharomyces*. *J. Cell Biol.* 98
45. Kilmartin, J. V., B. Wright, and C. Milstein. 1982. Rat monoclonal antitubulin antibodies derived by using a new nonsecreting rat cell line. *J. Cell Biol.* 93:576–582.
46. King, S. M., and J. S. Hyams. 1982. The mitotic spindle of *Saccharomyces cerevisiae*: assembly, structure and function. *Micron.* 13:93–117.
47. Koteliansky, V. E., M. A. Glukhova, M. V. Bejanian, A. P. Surguchov, and V. N. Smirnov. 1979. Isolation and characterization of actin-like protein from yeast *Saccharomyces cerevisiae*. *FEBS (Fed. Eur. Biochem. Soc.) Lett.* 102:55–58.
48. Lehtonen, E., and R. A. Badley. 1980. Localization of cytoskeletal proteins in preimplantation mouse embryos. *J. Embryol. Exp. Morphol.* 55:211–225.
49. Lillie, S. H., and J. R. Pringle. 1980. Reserve carbohydrate metabolism in *Saccharomyces cerevisiae*: responses to nutrient limitation. *J. Bacteriol.* 143:1384–1394.
50. Luna, E. J., V. M. Fowler, J. Swanson, D. Branton, and D. L. Taylor. 1981. A membrane cytoskeleton from *Dictyostelium discoideum*. I. Identification and partial characterization of an actin-binding activity. *J. Cell Biol.* 88:396–409.
51. Matile, P., H. Moor, and C. F. Robinow. 1969. Yeast cytology. *In* The Yeasts. Biology of Yeasts. A. H. Rose and J. S. Harrison, editors. Academic Press, Inc., New York. 1:219–302.
52. Moens, P. B., and E. Rapport. 1971. Spindles, spindle plaques, and meiosis in the yeast *Saccharomyces cerevisiae* (Hansen). *J. Cell Biol.* 50:344–361.
53. Neff, N. F., J. H. Thomas, P. Grisafi, and D. Botstein. 1983. Isolation of the β-tubulin gene from yeast and demonstration of its essential function *in vivo*. *Cell.* 33:211–219.
54. Ng, R., and J. Abelson. 1980. Isolation and sequence of the gene for actin in *Saccharomyces cerevisiae*. *Proc. Natl. Acad. Sci. USA* 77:3912–3916.
55. Nothnagel, E. A., L. S. Barak, J. W. Sanger, and W. W. Webb. 1981. Fluorescence studies on modes of cytochalasin B and phallotoxin action on cytoplasmic streaming in *Chara*. *J. Cell Biol.* 88:364–372.
56. Novick, P., and R. Schekman. 1983. Export of major cell surface proteins is blocked in yeast secretory mutants. *J. Cell Biol.* 96:541–547.
57. Oakley, B. R., and N. R. Morris. 1980. Nuclear movement is β-tubulin-dependent in *Aspergillus nidulans*. *Cell.* 19:255–262.
58. Paquin, C., and J. Adams. 1982. Isolation of sets of a, α, a/α, a/a, and α/α isogenic strains in *Saccharomyces cerevisiae*. *Curr. Genet.* 6:21–24.
59. Pesacreta, T. C., W. W. Carley, W. W. Webb, and M. V. Parthasarathy. 1982. F-actin in conifer roots. *Proc. Natl. Acad. Sci. USA* 79:2898–2901.
60. Peterson, J. B., and H. Ris. 1976. Electron-microscopic study of the spindle and chromosome movement in the yeast *Saccharomyces cerevisiae*. *J. Cell Sci.* 22:219–242.
61. Pringle, J. R., and L. H. Hartwell. 1981. The *Saccharomyces cerevisiae* cell cycle. *In* The Molecular Biology of the Yeast Saccharomyces: Life Cycle and Inheritance. J. N. Strathern, E. W. Jones, and J. R. Broach, editors. Cold Spring Harbor Laboratory, Cold Spring Harbor, NY. 97–142.
62. Pringle, J. R., and J.-R. Mor. 1975. Methods for monitoring the growth of yeast cultures and for dealing with the clumping problem. *Methods Cell Biol.* 11:131–168.
63. Pringle, J. R., K. Coleman, A. Adams, M. Kelley, R. Longnecker, and P. Oeller. 1982. Cellular morphogenesis in the yeast cell cycle. *J. Cell Biol.* 95(2, Pt. 2):24a. (Abstr.)
64. Quinlan, R. A., C. I. Pogson, and K. Gull. 1980. The influence of the microtubule inhibitor, methyl benzimidazol-2-yl-carbamate (MBC) on nuclear division and the cell cycle in *Saccharomyces cerevisiae*. *J. Cell Sci.* 46:341–352.
65. Robinow, C. F. 1975. The preparation of yeasts for light microscopy. *Methods Cell Biol.* 11:1–22.
66. Schekman, R. 1982. The secretory pathway in yeast. *Trends Biochem. Sci.* 7:243–246.
67. Schekman, R., and P. Novick. 1982. The secretory process and yeast cell-surface assembly. *In* The Molecular Biology of the Yeast Saccharomyces: Metabolism and Gene Expression. J. N. Strathern, E. W. Jones, and J. R. Broach, editors. Cold Spring Harbor Laboratory, Cold Spring Harbor, NY. 361–398.
68. Sherman, F., G. R. Fink, and J. B. Hicks. 1982. Methods in Yeast Genetics. (Laboratory manual.) Cold Spring Harbor Laboratory, Cold Spring Harbor, NY.

69. Shortle, D., J. E. Haber, and D. Botstein. 1982. Lethal disruption of the yeast actin gene by integrative DNA transformation. *Science (Wash. DC)*. 217:371–373.

70. Shriver, K., and L. Rohrschneider. 1981. Organization of pp60[src] and selected cytoskeletal proteins within adhesion plaques and junctions of Rous sarcoma virus-transformed rat cells. *J. Cell Biol.* 89:525–535.

71. Sloat, B. F., A. Adams, and J. R. Pringle. 1981. Roles of the *CDC24* gene product in cellular morphogenesis during the *Saccharomyces cerevisiae* cell cycle. *J. Cell Biol.* 89:395–405.

72. Spudich, A., and J. A. Spudich. 1979. Actin in Triton-treated cortical preparations of unfertilized and fertilized sea urchin eggs. *J. Cell Biol.* 82:212–226.

73. Strausberg, R. L., and P. S. Perlman. 1978. The effect of zygotic bud position on the transmission of mitochondrial genes in *Saccharomyces cerevisiae*. *Mol. Gen. Genet.* 163:131–144.

74. Sugrue, S. P., and E. D. Hay. 1981. Response of basal epithelial cell surface and cytoskeleton to solubilized extracellular matrix molecules. *J. Cell Biol.* 91:45–54.

75. Tilney. L. G. 1983. Interactions between actin filaments and membranes give spatial organization to cells. *In* Modern Cell Biology. Spatial Organization of Eukaryotic Cells. J. R. McIntosh, editor. Alan R. Liss, New York. 2:163–199.

76. Tilney, L. G., E. H. Egelman, D. J. DeRosier, and J. C. Saunders. 1983. Actin filaments, stereocilia, and hair cells of the bird cochlea. II. Packing of actin filaments in the stereocilia and in the cuticular plate and what happens to the organization when the stereocilia are bent. *J. Cell Biol.* 96:822–834.

77. Tkacz, J. S., and J. O. Lampen. 1972. Wall replication in Saccharomyces species: use of fluorescein-conjugated concanavalin A to reveal the site of mannan insertion. *J. Gen. Microbiol.* 72:243–247.

78. Tkacz, J. S., and J. O. Lampen. 1973. Surface distribution of invertase on growing *Saccharomyces* cells. *J. Bacteriol.* 113:1073–1075.

79. Water, R. D., J. R. Pringle, and L. J. Kleinsmith. 1980. Identification of an actin-like protein and of its messenger ribonucleic acid in *Saccharomyces cerevisiae*. *J. Bacteriol.* 144:1143–1151.

80. Wehland, J., M. Osborn, and K. Weber. 1979. Cell-to-substratum contacts in living cells: a direct correlation between interference-reflexion and indirect-immunofluorescence microscopy using antibodies against actin and α-actinin. *J. Cell Sci.* 37:257–273.

81. Wehland, J., M. Osborn, and K. Weber. 1980. Phalloidin associates with microfilaments after microinjection into tissue culture cells. *Eur. J. Cell Biol.* 21:188–194.

82. Wieland, T. 1977. Modification of actins by phallotoxins. *Naturwissenschaften.* 64:303–309.

83. Wieland, T., and H. Faulstich. 1978. Amatoxins, phallotoxins, phallolysin, and antamanide: the biologically active components of poisonous *Amanita* mushrooms. *CRC Crit. Rev. Biochem.* 5:185–260.

84. Wilkinson, L. E., and J. R. Pringle. 1974. Transient G1 arrest of *S. cerevisiae* cells of mating type α by a factor produced by cells of mating type *a*. *Exp. Cell Res.* 89:175–187.

85. Williamson, D. H., and D. J. Fennell. 1975. The use of fluorescent DNA-binding agent for detecting and separating yeast mitochondrial DNA. *Methods Cell Biol.* 12:335–351.

86. Wood, J. S., and L. H. Hartwell. 1982. A dependent pathway of gene functions leading to chromosome segregation in *Saccharomyces cerevisiae*. *J. Cell Biol.* 94:718–726.

87. Wulf, E., A. Deboben, F. A. Bautz, H. Faulstich, and T. Wieland. 1979. Fluorescent phallotoxin, a tool for the visualization of cellular actin. *Proc. Natl. Acad. Sci. USA* 76:4498–4502.